Langmuir-Blodgett films of gold nanorods with different silica shell thicknesses

E. Gergely-Fülöp[a], N. Nagy[a], A. Deák[a]*

[a] Institute for Technical Physics and Materials Science, Research Centre for Natural Sciences, HAS, P.0. Box 49, H-1525 Budapest, Hungary

*Corresponding author, deak@mfa.kfki.hu, Tel: +36 1 392 2602, Fax: +36 1392 2226

Abstract

We report the preparation and optical characterization of Langmuir- and Langmuir-Blodgett (LB) films of mesoporous silica coated gold nanorods with three different shell thicknesses. When measured in solution, the extinction of the particles in the short wavelength region becomes dominated by light scattering with increasing shell thickness. Due to the silica shell, however, it is possible to prepare continuous Langmuir and Langmuir-Blodgett monolayers of the particles over macroscopic areas. To investigate the role of the gold core and the silica coating in the optical properties of the monolayers, reflection measurements in combination with thin-film optical modeling were carried out. Interestingly, the optical behavior of the Si deposited LB monolayers is mainly governed by the silica shell: the reflection spectrum is dominated by thin-film interference instead of the localized surface plasmon resonance peaks. This is in agreement with our earlier results obtained for core-free plain silica nanoparticle LB monolayers.

Keywords: gold nanoparticle; core/shell nanoparticle; Langmuir-Blodgett film; optical property; plasmonics

1. Introduction

The importance of wet chemical synthesis of inorganic structures owning at least one dimension at the nanoscale has been a continuously emerging topic in the last two decades. A high variety of methods have been developed synthesizing various types of nanoparticles [1–4] and thin films [5–9] for different purposes.

Plasmonic gold nanoparticles gained immense attention in recent past due to their special optical properties. These small noble metal nanoparticles can support certain localized surface plasmon resonance modes that results in a very large extinction (absorption plus scattering) cross-sections and near-field enhancements at certain wavelength [10]. There are many literature reports about how to control the optical properties of these particles through adjusting their size and shape during wet-chemical nanoparticle growth. Based on the specific interaction of the nanoparticles with light, applications in the field of cancer therapy [11], sensor applications [12] and energy conversion [13] are envisaged. Besides of the optical properties, however, the physic chemical behavior of the particles is crucial. Due to their size the particles belong to the colloidal domain, and their interaction with other substances is governed by colloidal interactions. These often determine or limit the range of possible applications (e.g. due to aggregation or unwanted surface adsorption).

In this paper we focus on the connection between the physico-chemical and optical properties of gold/mesoporous silica core/shell nanoparticles as well as their assembled structures. We investigate how an increasing thickness of silica shell affects the extinction spectrum of the nanoparticles in solution and when deposited in the form of a monolayer on a solid support.

2. Materials and methods

2.1 Materials

Sodium borohydride, ReagentPlus® 99 % (NaBH4); tetrachloroauric (III) acid trihydrate, ACS reagent ($HAuCl_4 \bullet 3H_2O$); cetyltrimethyl ammonium bromide, SigmaUltra 99 % (CTAB); tetraethyl ortosilicate, puriss, 99 % (TEOS); L-ascorbic acid, ACS reagent 99 %; silver nitrate, 99.9999 % metal basis ($AgNO_3$) and methanol, puriss. p.a. (max. 0.005 % H_2O) were purchased from Sigma-Aldrich. Ammonium hydroxide, 32 % from Scharlau, Sodium hydroxide, a.r. (NaOH) from Reanal and chloroform, ultra-resi analyzed, 99.8 %, from J. T. Baker were used. All chemicals were used as received. For all experiments ultrapure water with a resistivity of 18.2 MΩ/cm was used.

2.2 Nanoparticle synthesis

Gold/silica core/shell nanorods were synthetized similarly as reported by us earlier [14] according to the procedure in [15]. First, 5 ml 0.5 mM $HAuCl_4$ was mixed with 5 ml 0.2 M CTAB, then 600 µl 0.01 M ice-cold $NaBH_4$ was added. The resulting brownish seed solution was vigorously stirred for 30 s, which was followed by a slow stirring for 15 minutes at 50 °C. To get the nanorods, 3 ml of the seed solution was added under stirring to a growth solution containing 50 ml 1 mM $HAuCl_4$, 50 ml 0.2 M CTAB, 100 µl 0.04 M $AgNO_3$ and 700 µl 0.1 M ascorbic acid and then left undisturbed for a night at 30 °C. These CTAB-capped nanorods were in a single step coated with a mesoporous silica shell according to literature, resulting in disordered pores in the silica coating with ca. 4 nm diameter and ca. 2 nm wall thickness [15]. To coat the nanorods, 15 ml of the as-synthesized nanorod sol was centrifuged at 7500 rpm for 30 min and redispersed in 10 ml of water. The pH was adjusted to

~10-11 using 100 µl 0.1 M NaOH. Under magnetic stirring, 3x30 µl 20 % TEOS in MeOH was injected into the reaction vessel at 30 minute intervals to coat the gold nanorods with a 15 nm thick silica shell. The samples were subjected to repeated centrifugation and redispersion in methanol (6 times) to remove the positively charged surfactant molecules until a zeta-potential value about -30 mV was reached, and small residual core-free silica particles were also removed. To obtain thicker silica shells, the resulting, purified sols are concentrated from 15 ml to 8 ml and to this solution, 2 ml 15 % NH_3 in H_2O was added. Then, to get 50 nm thick shell, 3x15 µl TEOS was added in 3 hour intervals. After this step, the solution was centrifuged again to remove small silica particles and residual NH_3, then the resulting solution can be used to increase silica shell thickness to 80 nm with 4x15 µl TEOS again with 3 hour intervals. The resulting sol can be purified again by repeated centrifugation. For the film preparation the particles were used without any further surface-modification.

2.3 Langmuir-Blodgett film preparation

Silicon substrates were washed with acetone, water, 2 % hydrofluoric acid solution and finally with water. Glass slides (Menzel Gläser microscope slides, AA00000102E) were washed with ethanol and water. To spread the nanoparticles at the air/water interface in a Langmuir-trough (KSV2000), the particles dispersed in methanol were diluted with chloroform (1:2 volume ratio) and sonicated for 5 minutes right before spreading. The nanoparticles were spread at the water/air interface using a Hamilton syringe. After 10 minutes, when chloroform evaporated, the particles were compressed with a barrier speed of 0.4 cm^2/s. As the surface pressure reached the value of ca. 1 mN/m, the compression speed was lowered to 0.2 cm^2/s. The Langmuir-Blodgett (LB) films were prepared by vertical deposition (4 mm/min), at ca. 80 % of the collapse pressure.

2.4 Characterization techniques

The zeta-potential of the particles was estimated using electrophoretic light scattering technique (Malvern Zetasizer Nano ZS). The particle size and the shell thickness were measured using a Philips CM20 transmission electron microscope (TEM). LB-film morphology deposited on Si substrates was investigated using a LEO 1540 XB field emission scanning electron microscope (SEM) with an acceleration voltage of 5.00 kV. The optical properties of the sols were studied using UV-Vis spectroscopy (Agilent 8453). LB-films transferred onto Si substrates were measured optically in reflection geometry using an Avantes AvaSpec-2048 fiber coupled spectrometer in the 450-950 nm wavelength range. For determining the film's structure detailed optical modelling was performed using the wvase32 software [16].

3. Results and discussion

3.1 Properties of the synthesized nanoparticles

Figure 1 shows representative TEM images of the synthesized nanoparticles. The size of the gold nanorod cores measures 23 nm × 40 nm, and 21 nm × 35 nm, respectively. The silica coating on all nanoparticles is continuous, the shell thickness varies between 15 nm and 80 nm depending on the amount of TEOS added during the growth of the shell. Increasing TEOS addition results in a thicker silica shell. Although not visible on these images, the deposited shell is mesoporous, as was confirmed by us and other groups earlier [14, 15, 17]. The silica deposition on the CTAB bilayer at the gold nanorod surface results in a mesoporous

shell, where the characteristic pore diameter is around 4 nm with a wall thickness of 2 nm [15].The channels span over the whole shell thickness and are oriented perpendicular to the surface of the nanorod [18,19]. Due to the optimized centrifuging procedure performed after the shell growth, there are no core-free small mesoporous silica nanoparticles present in the samples.

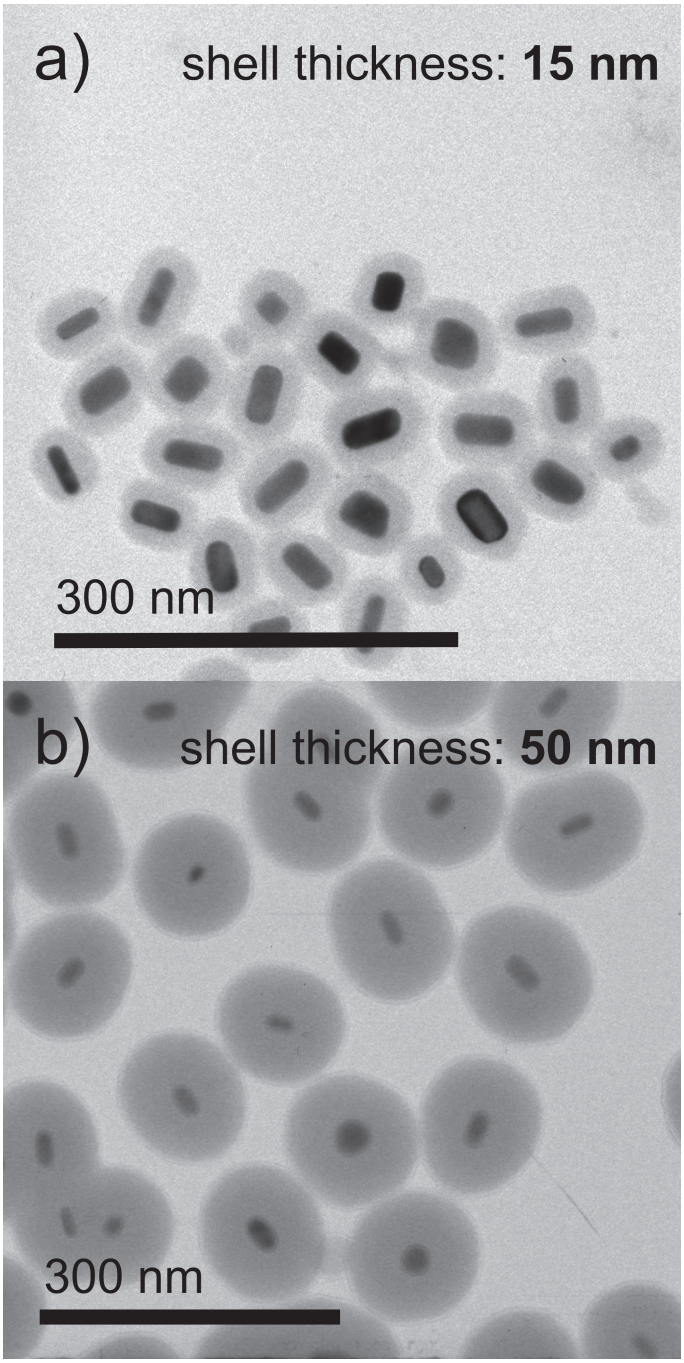

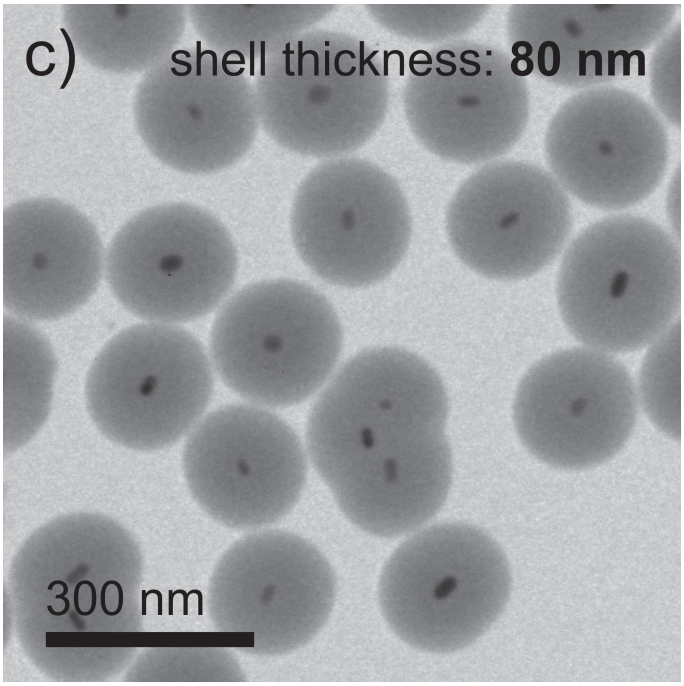

Fig. 1 TEM images of the gold-silica core-shell nanorods with different shell thicknesses (15 nm 50 nm and 80 nm, respectively). Note, that the (a), (b), (c) images correspond to the spectra in Figure 2.a, 2.b, and 2.c, respectively. Scale bar: 300 nm for all images.

When investigating the optical properties of the nanoparticles using visible spectroscopy (Figure 2), both the plasmonic properties of the gold nanorod cores and the effect of the different shell thickness on the extinction spectra can be observed. The spectra feature two main extinction peaks independently from the thickness of the shell and can be attributed to the two characteristic localized surface plasmon resonance modes that are supported by the gold cores. The peak at longer wavelengths (615-625 nm) featuring higher intensity can be assigned to the longitudinal mode, whereas the small peak around 525 nm belongs to the transversal mode. In the spectra of the nanorods with the thinnest (15 nm) silica shell (Figure 2.a) no significant deviation from the extinction spectrum of the starting nanorod can be observed. For the thicker silica shells (50 and 80 nm), however, there is a striking difference between the spectra before and after the silica coating. This difference refers to an increased extinction at shorter wavelengths compared to the original spectrum of the as-prepared nanorods. For the nanoparticle sample with the thickest shell, the extinction around 400 nm already exceeds the intensity of the longitudinal plasmon peak. The shell and wavelength dependent extinction increase can be attributed to the increasing scattering of the particles with increasing overall particle size. The scattering causes an increasing extinction with decreasing wavelength that is superimposed on the original particle spectrum. It is important to point out, however, that this superposition does not result in a simple addition of the optical damping caused by the scattering due to size and extinction due to plasmon resonance. Especially for the largest shell thickness (Figure 2.c) it is clear that the transversal plasmon resonance peak almost “disappears” in the short wavelength tail of the spectrum; this part of the spectrum is dominated by Rayleigh scattering.

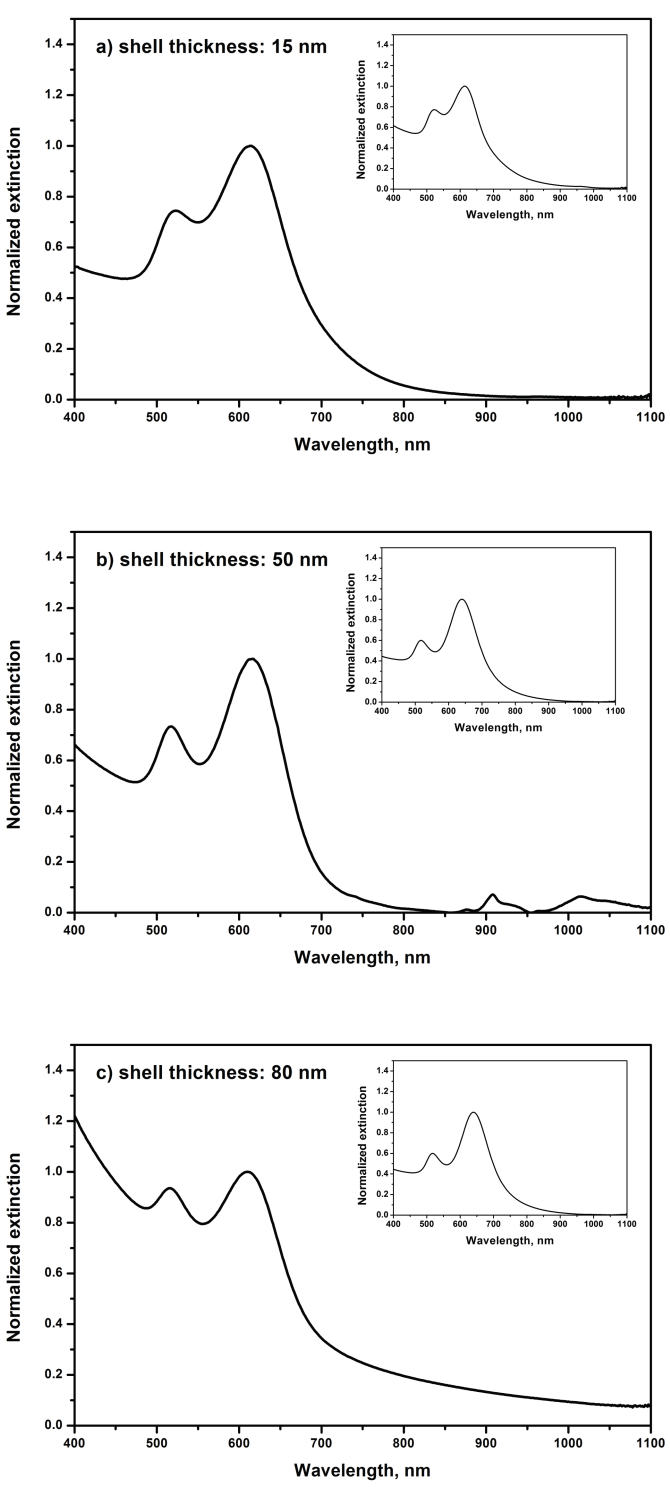

Fig. 2 Normalized extinction spectra of the three different sols of silica-coated gold nanorods with different shell thicknesses (in water): a) 15 nm, b) 50 nm and c) 80 nm. The insets show the measured spectrum of the gold nanorod sols before the silica-coating procedure.

3.2 Properties of Langmuir- and Langmuir-Blodgett films

Independently of the silica shell thickness, all particle types could be spread at the air/water interface as demonstrated earlier by us for another particle type [14]. After the evaporation of

the spreading solvent the particles were trapped at the interface. This enabled to record their surface pressure – area isotherm (Figure 3). The surface pressure is zero over a large area decrease at the beginning of the compression, indicating a contamination free interface. After decreasing the area below the contact area, a sudden increase of the surface pressure can be observed. At this point the presence of the Langmuir film can be observed even by naked eye with a weak color corresponding to the color of the nanoparticle solutions. The collapse pressure values are around 25 mN/m. This value is similar to that of Stöber silica particles of comparable diameter [20].

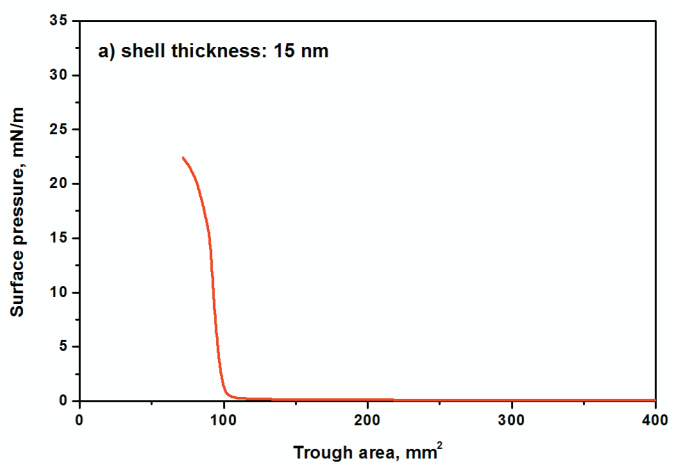

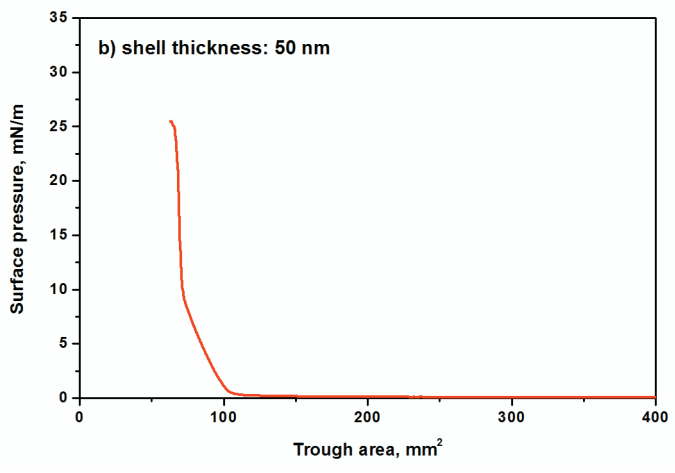

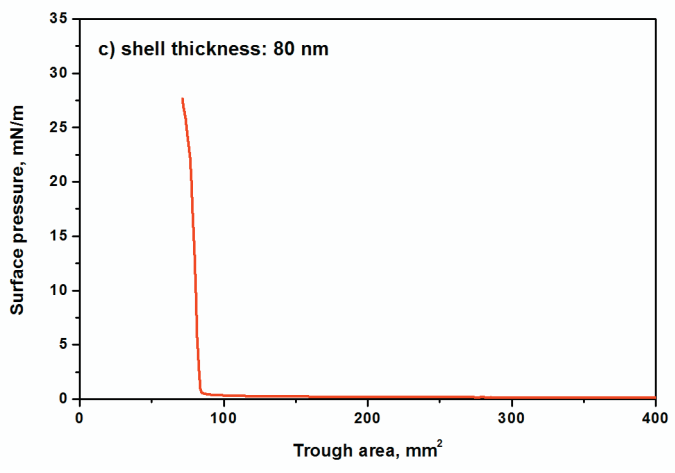

Fig.3 Surface pressure vs. area isotherms of the three different core-shell nanoparticle systems, with a) 15 nm, b) 50 nm and c) 80 nm silica shell thicknesses.

After the transfer of the Langmuir-film onto silicon substrates the LB-films seem also continuous and defect-free on the macroscopic scale. The SEM investigations showed that the resulting LB-films are compact monolayers (Fig. 4). Hexagonally closed packed ordering can be found only in case of the largest shell thickness on some areas of the sample. This is due to the fact that with increasing silica shell thickness the shape of the core-shell structure approaches more and more that of a sphere. For smaller shell thicknesses the film is disordered, side-by-side ordering cannot be seen as typical for high aspect ratio, shell-free nanorods [21, 22, 23]. It is also worth to note that for particles with shell thickness of 15 nm and 50 nm the secondary electron flux provided by the gold cores can escape through the silica shell and reach the detector. This is the reason why the gold nanorod cores are clearly visible in Figure 4.a and can be perceived in Figure 4.b.

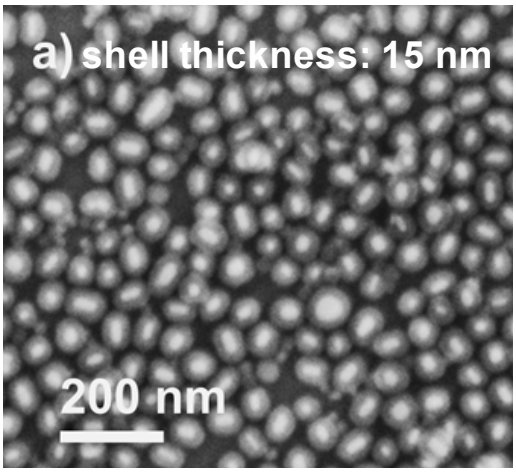

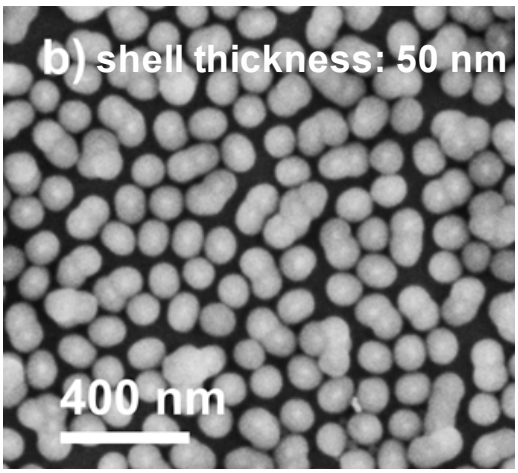

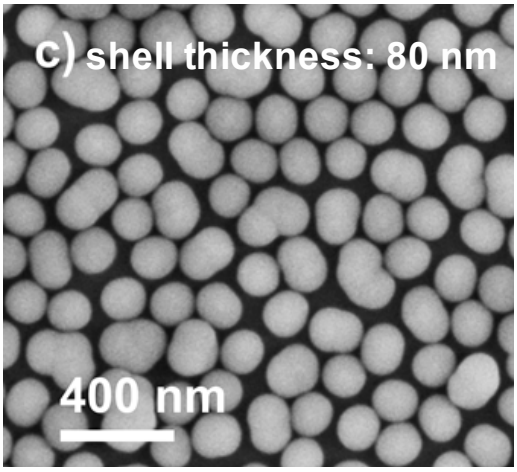

Fig. 4 SEM images of Langmuir-Blodgett films composed from gold-silica core-shell nanorods with the shell thickness of 15 nm, 50 nm, and 80 nm, respectively.

The optical spectroscopic characterization of the LB-films was carried out in reflection geometry at normal incidence in the wavelength range of 450-950 nm (Figure 5). An uncoated Si wafer was used as reference. The characteristic longitudinal plasmon resonance peaks of the nanorods (Figure 5.a-5.c) are clearly observable in the reflection spectrum of the LB monolayers, resulting in a small local reflection minimum between 615 nm and 625 nm depending on the shell thickness of the nanoparticles. Nevertheless all of the monolayers show intensive colors when observed by naked eye. In order to shed light on the details of the optical behavior of the core/shell monolayers, we performed additional optical modeling.

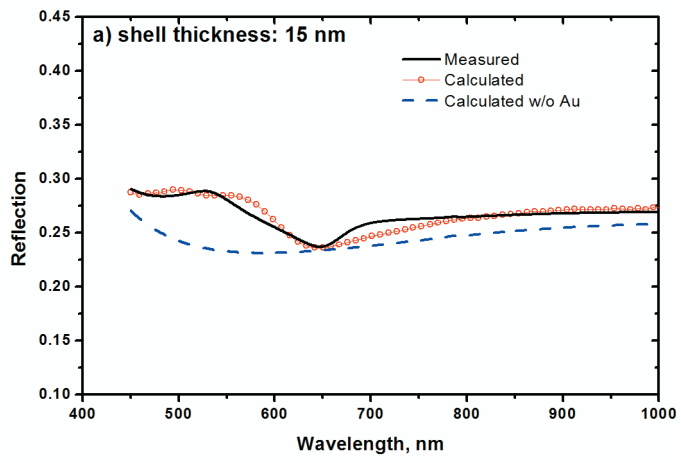

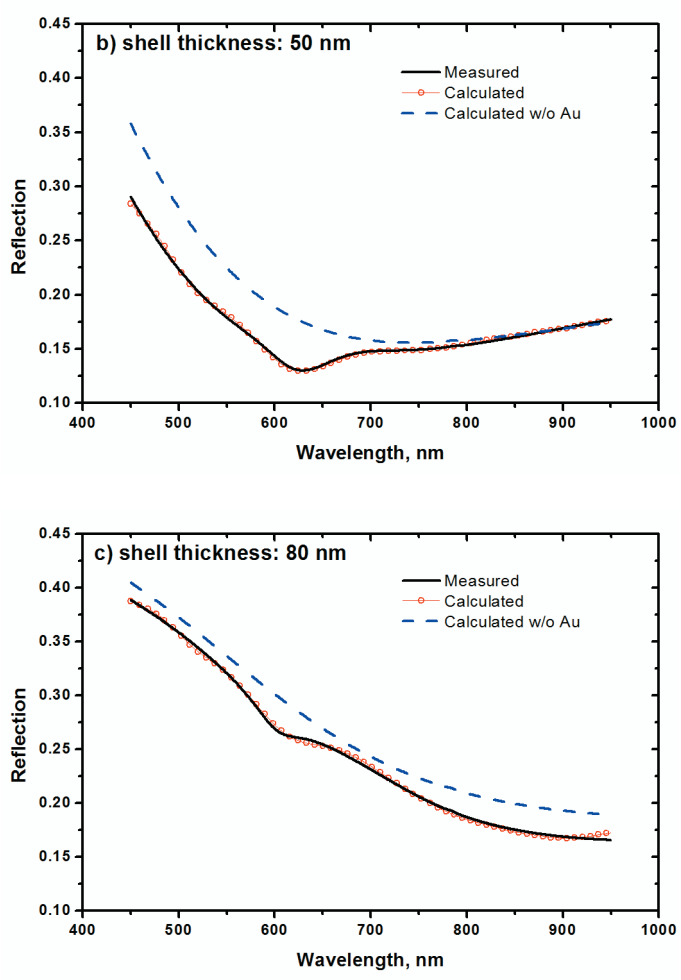

Fig. 5 Measured and calculated reflectance spectra of the LB monolayers on Si substrates composed from gold/silica core/shell nanorods with different shell thicknesses (a) 15 nm, b) 50 nm, c) 80 nm). In order to demonstrate the optical role of the gold cores, the reflection spectra plotted with dashed lines were calculated by substituting gold with silica in the optical model of the corresponding sample (w/o Au).

The optical models were built up according to the schematics in Figure 6 and makes use of the Bruggeman effective medium approximation (EMA) [24], that allows to treat complex multicomponent layers as a single, optically homogeneous layer. The LB-films were divided into three stratified layers in the z-axis perpendicular to the substrate (light propagation direction): the first layer was composed from silica and void applying EMA. The second layer corresponds to the gold core particle region containing also gold, silica and void. Obviously, the optical properties of gold nanoparticles differ from bulk gold and this difference has to be taken into account. An appropriate and widely used solution is to treat the optical response of the particles as combination of oscillator models: typically one Drude- and three Lorentz oscillators are used [25, 26, 27]. The third layer in the stack is similar to the first but not the same: the non-uniformity and the polydispersity of the particulate system result here a bit higher effective layer thickness and void ratio. Fitting the layer thickness values, the ratios of materials, and the oscillator parameters the reflection spectra can be calculated.

The fitted reflection curves are shown in Figure 5 with empty symbols. The good agreement between the experimental and simulated spectra allows us to retrieve the shell thickness of the particles, which corresponds to the thickness of the lowest laying EMA layer in our optical model. The obtained shell thickness values are 15.1 nm, 47.5 nm, and 84.4 nm,

respectively. These values are in very good agreement with that resulted from the TEM analysis.

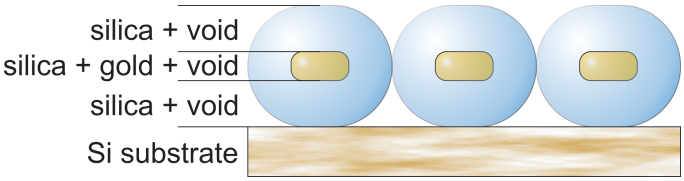

Fig. 6 Schematics of the optical model: the LB-films were divided into three slices and in every slice the Bruggeman effective medium approximation was applied.

Compared to the rather flat reflection spectrum in Figure 5.a, for particle samples with ca. 50 nm (Figure 5.b) and 80 nm (Figure 5.c) shell thickness a strong overall wavelength modulation of the spectrum can be observed. This we attribute to the thin film interference arising from the LB monolayers that get more pronounced as the overall size of the core/shell particles increases. This behavior has been previously shown to apply to the LB mono- and multilayers of Stöber-silica nanoparticles [28, 29]. In order to verify this assumption, we performed additional reflection spectra calculation. After obtaining the optical model parameters from the reflection spectra fitting described above, we replaced the gold in the optical model with silica. Reflection spectra calculations were hence carried out assuming plain silica particles without gold cores (w/o Au) but with identical size compared to the core/shell particles (Figures 5.a-c, dashed lines). The result of the simulation is plotted in Figure 5.a-5.c using dashed lines. It is clear, that as the shell thickness increases, the overall wavelength dependent reflection of the monolayer becomes dominated by thin film interference. The fairly good agreement between the experimental spectra (solid lines) and the calculated trends (dashed line) agree very well with previous result obtained for core-free plain silica particles [28, 29], i.e., in the compact LB layer no significant scattering arises from the individual nanoparticles.

Conclusion

We have shown that increasing the shell thickness of gold nanorod/mesoporous silica core/shell nanoparticles significantly alters the optical properties of the system, whereas not affecting its physico-chemical behavior. In solution the increasing shell thickness results in an enhanced Rayleigh scattering from the particles, suppressing the plasmon resonance of the particles gradually. The Langmuir-Blodgett monolayers of the particles, however do not suffer from the increased scattering due to the close packed nature of the films. Although plasmon resonance in the monolayer can be still observed up to a silica shell thickness of 80 nm, the reflection spectra are being dominated by the thin film interference corresponding to the optical response of closely packed dielectric nanospheres. Shell thickness values above 15 nm significantly alter the optical response of the nanoparticle systems in solution and on substrate and hence might limit the applicability of core shell particles with a thick mesoporous silica shell, e.g., in high temperature applications, where thick shell can effectively stabilize anisometric plasmonic nanoparticles [17].

Acknowledgement

This work received funding from the Hungarian Scientific Research Fund (OTKA-PD-105173). András Deák acknowledges the support from the János Bolyai research fellowship.

The help of György Sáfrán with the TEM and János Volk with the SEM images is appreciated.

References

[1] Panigrahi, S., Basu, S., Praharaj, S., Pande, S., Jana, S., Pal, A., Ghosh, S.K., Pal, T., "Synthesis and Size-Selective Catalysis by Supported Gold Nanoparticles: Study on Heterogeneous and Homogeneous Catalytic Process", "Journal of Physical Chemistry C", 111(12), (2007), 4596–4605
http://dx.doi.org/10.1021/jp067554u
DOI: 10.1021/jp067554u

[2] Iskandar, F., "Nanoparticle processing for optical applications – A review", "Advanced Powder Technology", 20(4), (2009), 283–292
http://dx.doi.org/10.1016/j.apt.2009.07.001
DOI: 10.1016/j.apt.2009.07.001

[3] Shchukin, D.G., Sukhorukov, G.B., "Nanoparticle Synthesis in Engineered Organic Nanoscale Reactors", "Advanced Materials", 16(8), (2004), 671–682
http://dx.doi.org/10.1002/adma.200306466
DOI: 10.1002/adma.200306466

[4] Chen, H., Zhen, Z., Todd, T., Chu, P.K., Xie, J., "Nanoparticles for improving cancer diagnosis", "Materials Science and Engineering: R: Reports", 74(3), (2013), 35–69
http://dx.doi.org/10.1016/j.mser.2013.03.001
DOI: 10.1016/j.mser.2013.03.001

[5] Hench, L. L., West, J. K., "The sol-gel process", "Chemical Reviews", 90(1), (1990), 33-72
http://dx.doi.org/10.1021/cr00099a003
DOI: 10.1021/cr00099a003

[6] Brinker, C. J., Hurd, A. J., Schunk P. R., Frye, G. C., Ashley, C. S., "Review of sol-gel thin film formation", "Journal of Non-Crystalline Solids", 147-148, (1992), 424-436
http://dx.doi.org/10.1016/S0022-3093(05)80653-2
DOI: 10.1016/S0022-3093(05)80653-2

[7] Wang, D., Bierwagen, G. P., "Sol-gel coatings on metals for corrosion protection", "Progress in Organic Coatings", 64(4), (2009), 327-338
http://dx.doi.org/10.1016/j.porgcoat.2008.08.010
DOI: 10.1016/j.porgcoat.2008.08.010

[8] Volentiru, E., Nyári, M., Szabó, G., Hórvölgyi, Z., Muresan, L. M., "Silica sol-gel protective coatings against corrosion of zinc substrates", "Periodica Polytechnica Chemical Engineering", 58(Sup), (2014), 61-66
http://dx.doi.org/10.3311/PPch.7302
DOI: 10.3311/PPch.7302

[9] Detrich, Á., Nyári, M., Volentiru, E., Hórvölgyi, Z., "Estimation of contact angle for hydrophobic silica nanoparticles in their hexagonally ordered layer", "Materials Chemistry and Physics", 140(2-3), (2013), 602-609

http://dx.doi.org/10.1016/j.matchemphys.2013.04.013
DOI: 10.1016/j.matchemphys.2013.04.013

[10] Noguez, C., "Surface Plasmons on Metal Nanoparticles: The Influence of Shape and Physical Environment", "Journal of Physical Chemistry C", 111(10), (2007), 3806–3819
http://dx.doi.org/10.1021/jp066539m
DOI: 10.1021/jp066539m

[11] Liu, X., Huang, N., Li, H., Wang, H., Jin, Q., Ji, J., "Multidentate polyethylene glycol modified gold nanorods for in vivo near-infrared photothermal cancer therapy", "ACS Applied Materials & Interfaces", 6(8), (2014), 5657–5668
http://dx.doi.org/10.1021/am5001823
DOI: 10.1021/am5001823

[12] Vigderman, L., Khanal, B.P., Zubarev, E.R., "Functional Gold Nanorods: Synthesis, Self-Assembly, and Sensing Applications", "Advanced Materials", 24(36), (2012), 4811–4841
http://dx.doi.org/10.1002/adma.201201690
DOI: 10.1002/adma.201201690

[13] Kozanoglu, D., Apaydin, D.H., Cirpan, A., Esenturk, E.N., "Power conversion efficiency enhancement of organic solar cells by addition of gold nanostars, nanorods, and nanospheres", "Organic Electronics", 14(7), (2013), 1720–1727
http://dx.doi.org/10.1016/j.orgel.2013.04.008
DOI: 10.1016/j.orgel.2013.04.008

[14] Fülöp, E., Nagy, N., Deák, A., Bársony, I., "Langmuir–Blodgett films of gold/silica core/shell nanorods", "Thin Solid Films", 520(23), (2012), 7002–7005
http://dx.doi.org/10.1016/j.tsf.2012.07.097
DOI: 10.1016/j.tsf.2012.07.097

[15] Gorelikov, I., Matsuura, N., "Single-step coating of mesoporous silica on cetyltrimethyl ammonium bromide-capped nanoparticles", "Nano Letters", 8(1), (2008), 369-373
http://dx.doi.org/10.1021/nl0727415
DOI: 10.1021/nl0727415

[16] http://www.jawoollam.com/wvase.html

[17] Gergely-Fülöp, E., Nagy, N., Deák, A., "Reversible shape transition: Plasmonic nanorods in elastic Nanocontainers", "Materials Chemistry and Physics", 141(1), (2013), 343-347
http://dx.doi.org/10.1016/j.matchemphys.2013.05.020
DOI: 10.1016/j.matchemphys.2013.05.020

[18] Chen, J., Zhang, R., Han, L., Tu, B., Zhao, D., "One-pot synthesis of thermally stable gold@mesoporous silica core-shell nanospheres with catalytic activity", "Nano Research", 6(12), (2013), 871-879
http://dx.doi.org/10.1007/s12274-013-0363-1
DOI: 10.1007/s12274-013-0363-1

[19] Yang, J., Zhang, F., Chen, Y., Qian, S., Hu, P., Li, W., Deng, Y., Fang, Y., Han, L., Luqman, M., Zhao, D., "Core-shell Ag@SiO2@mSiO2 mesoporous nanocarriers for metal-enhanced fluorescence", "Chemical Communications", 47(42), (2011), 11618-11620
http://dx.doi.org/10.1039/C1CC15304H
DOI: 10.1039/C1CC15304H

[20] Deák, A., Hild, E., Kovács, A. L., Hórvölgyi, Z., "Contact angle determination of nanoparticles: film balance and scanning angle reflectometry studies", "Physical Chemistry Chemical Physics", 9(48), (2007), 6359-6370
http://dx.doi.org/10.1039/B702937N
DOI: 10.1039/B702937N

[21] Kim, F., Kwan, S., Akana, J., Yang, P. D., "Langmuir-Blodgett nanorod assembly", "Journal of the American Chemical Society", 123(18), (2001), 4360-4361
http://dx.doi.org/10.1021/ja0059138
DOI: 10.1021/ja0059138

[22] Yang, P.D., Kim, F., "Langmuir–Blodgett assembly of one-dimensional nanostructures", "A European Journal of Chemical Physics and Physical Chemistry", 3(6), (2002), 503-503
http://dx.doi.org/10.1002/1439-7641(20020617)3:6<503::AID-CPHC503>3.0.CO;2-U
DOI: 10.1002/1439-7641(20020617)3:6<503::AID-CPHC503>3.0.CO;2-U

[23] Tao, A., Kim, F., Hess, C., Goldberger, J., He, R. R., Sun, Y. G., Xia, Y. N., Yang, P. D., "Langmuir−Blodgett silver nanowire monolayers for molecular sensing using surface-enhanced Raman spectroscopy", "Nano Letters", 3(9), (2003), 1229-1233
http://dx.doi.org/10.1021/nl0344209
DOI: 10.1021/nl0344209

[24] Nagy, N., Deák, A., Hórvölgyi, Z., Fried, M., Agod, A., Bársony, I., "Ellipsometry of Silica nanoparticulate Langmuir−Blodgett films for the verification of the validity of effective medium approximations", "Langmuir", 22(20), (2006), 8416-8423
http://dx.doi.org/10.1021/la061259j
DOI: 10.1021/la061259j

[25] Loncaric, M., Sancho-Parramon, J., Zorc, H., "Optical properties of gold island films—a spectroscopic ellipsometry study", "Thin Solid Films", 519(9), (2011), 2946-2950
http://dx.doi.org/10.1016/j.tsf.2010.12.068
DOI: 10.1016/j.tsf.2010.12.068

[26] Oates, T. W. H., Wormeester, H., Arwin, H., "Characterization of plasmonic effects in thin films and metamaterials using spectroscopic ellipsometry", "Progress in Surface Science", 86(11-12), (2011), 328–376
http://dx.doi.org/10.1016/j.progsurf.2011.08.004
DOI: 10.1016/j.progsurf.2011.08.004

[27] Losurdo, M., Bergmair, M., Bruno, G., Cattelan, D., Cobet, C., de Martino, A., Fleischer, K., Dohcevic-Mitrovic, Z., Esser, N., Galliet, M., Gajic, R., Hemzal, D., Hingerl, K., Humlicek, J., Ossikovski, R., Popovic, Z. V., Saxl, O., "Spectroscopic ellipsometry and

polarimetry for materials and systems analysis at the nanometer scale: state-of-the-art, potential, and perspectives", "Journal of Nanoparticle Research", 11(7), (2009), 1521-1554
http://dx.doi.org/10.1007/s11051-009-9662-6
DOI: 10.1007/s11051-009-9662-6

[28] Deák, A., Székely, I., Kálmán, E., Keresztes, Zs., Kovács, A. L., Hórvölgyi, Z., "Nanostructured silica Langmuir–Blodgett films with antireflective properties prepared on glass substrates", "Thin Solid Films", 484(1-2), (2005), 310-317
http://dx.doi.org/10.1016/j.tsf.2005.01.096
DOI: 10.1016/j.tsf.2005.01.096

[29] Deák, A., Bancsi, B., Tóth, A. L., Kovács, A. L., Hórvölgyi, Z., "Complex Langmuir–Blodgett films from silica nanoparticles: An optical spectroscopy study", "Colloids and Surfaces A: Physicochemical and Engineering Aspects", 278(1-3), (2006), 10-16
http://dx.doi.org/10.1016/j.colsurfa.2005.11.070
DOI: 10.1016/j.colsurfa.2005.11.070